URSI AP-RASC 2019, New Delhi, India, 09 - 15 March 2019

Estimation of Transmitted Power Density from Temperature Experiment for EMF Exposure Assessment at 60 GHz

Kun Li[(1)], Kengo Kawabata [(1) (2)], Kensuke Sasaki [(1)], Ryosuke Suga [(2)], Soichi Watanabe [(1)], and Osamu Hashimoto[(2)]
(1) National Institute of Information and Communications Technology, Nukuikitamachi 4-2-1, Koganei, Tokyo, 184-8795 Japan
(2) Department of Electrical Engineering and Electronics, Aoyama Gakuin University, 5-10-1 Fuchinobe, Chuo-ku, Sagamihara-shi, Kanagawa, 252-5258, Japan

Abstract

This study aims to develop an experimental approach to estimate the transmitted power density inside human body for dosimetry study of millimeter wave exposure. We developed a temperature measurement system comprised of a millimeter wave generation apparatus at 60 GHz, a semi-solid glycerin phantom and an infrared camera. Based on this system, an estimation method of transmitted power densities was proposed by analyzing the temporal trend of temperature elevation on phantom surface. The validity of the proposed method was confirmed for the case of using a standard horn, and some results of using multi-element patch array antennas were demonstrated.

1. Introduction

Millimeter wave (MMW) frequencies are promising for wireless communication system owing to the large usable bandwidth and potential high data rate, such as 5G and WiGig (Wireless Gigabit) [1]. In particular, 60 GHz band is now commercially available in WiGig system. On the other hand, such high frequency wireless devices utilized in human vicinity increase public concerns on human exposure to electromagnetic fields (EMF).

International safety standards and guidelines have been established by IEEE [2] and ICNIRP [3], where the incident power density is used as a dosimetric quantity instead of SAR (specific absorption rate) for MMW exposure assessment over 3 GHz [2] and 10 GHz [3]. However, due to the reflection phenomenon at the skin surface, incident power density does not always represent the thermal effects caused by MMW exposure since it is a physical quantity outside the human body. Although, previous study has reported the correlation between incident power density and skin temperature rise [4], the energy absorbed by the human body varies depending on many parameters, such as the antenna radiation pattern, incident wave angle and the polarization. In order to prevent an excessive skin heating due to the human exposure to electromagnetic waves at MMW bands, an evaluation index inside the human body that highly correlated with the skin surface temperature elevation is needed.

Recently, exposure safety guidelines [5] published new drafts, where the major revision is that the new safety guidelines consider the use of new dosimetric limits in MMW frequency region, defined as the transmitted power density [5]. However, owing to a shallow penetration depth within 1 or 2 mm at MMW frequencies, transmitted power density inside the human skin cannot be measured directly using an E-field probe as that in a SAR experiment. In general, analytical method is used to investigate the worst case of EMF exposure at MMW frequency region. In addition, in experimental approach, it is relatively difficult to conduct the dosimetry study in consideration of actual complicated exposure conditions (human body shape and antenna near-field). Therefore, it is indispensable to develope a measurement method that enables quantitative evaluation of transmitted power density assuming actual exposure conditions.

This paper presents an experimental method to derive the maximum transmitted power density from the measured results of surface temperature elevation using a skin-equivalent phantom. The results show that the transmitted power density estimated by the thermal experiment data agree well with the analytical outcomes, indicating the validity of the proposed method.

2. Measurement System of Temperature Elevation using a Phantom at 60 GHz

Thermography method is a conventional approach to evaluate the power absorption by microwave exposure, where a temperature image on tissue surface can be detected using an infrared camera after the exposure is stopped. However, in millimeter wave frequencies, radio wave energy is mainly absorbed within the surface tissue. This will result in a rapid heat transfer from skin to the air. Thus, the improvement of the measurement accuracy and repeatability of the temperature measurement is crucial for the estimation of the transmitted power density in the MMW region.

Figure 1 shows the measurement system of temperature elevation experiment [6]. A semi-solid glycerin phantom with a dielectric property close to human skin at 60 GHz was utilized, as shown in Table 1. An infrared camera (H8000, Avio) was used to continuously detect and record the temperature elevation data on the phantom surface with an observation angle of 40 degrees. The maximum value of the surface temperature rise was measured from the difference between the initial state temperature and the maximum temperature after 1800 seconds exposure. The distance from the antenna aperture to the phantom surface was fixed at d = 60 mm. The phantom was exposed to MMWs from several representative antennas at the normal incidence angle with an input power normalized to 1 W.

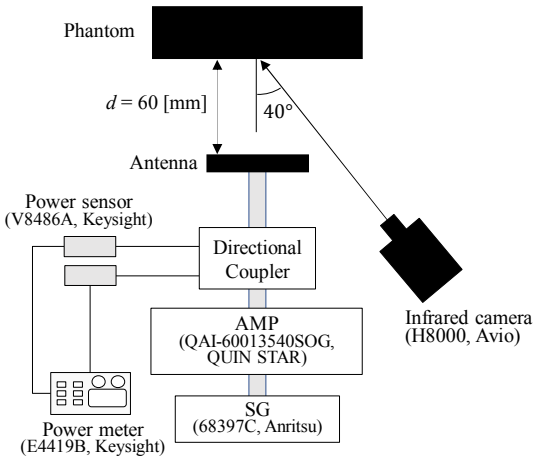

Figure 1. Measurement system of temperature elevation using a phantom with an infrared camera at 60 GHz.

Table 1. Parameters of glycerin phantom used in thermal experiment.

Size: $x \times y \times z$ [mm]	98 × 98 × 28
Relative permittivity: ε_r	6.6
Conductivity: σ [S/m]	21
Thermal conductivity: κ [W/(m◦C)]	0.5
Mass density: ρ [kg/m^3]	1100
Specific heat: c [J/(kg◦C)]	3300

3. Estimation Method of Maximum Transmitted Power Density

As discussed in the previous study [7], it is reasonable that the time evolution of the temperature on the skin surface exposed to the MMWs follows a primary delay function, as expressed by an approximation equation,

$$T(t) = T_{max}\left(1 - e^{-\frac{t}{\tau}}\right) \quad (1)$$

where T_{max} denotes the maximum temperature elevation. τ shows the thermal time constant. In the early stage of exposure, the initial temperature rise distribution depends on the spatial gradient of the SAR distribution. In (1), the instantaneous temperature at the time of the time constant ($t = \tau$) represents 63% of the maximum temperature elevation value. When $t > \tau$, $T(t)$ increases close to the maximum temperature T_{max}. This indicates that the temperature increase from $T(t = 0)$ to $T(t = \tau)$ is reasonably correlating with the total energy absorption caused by the electromagnetic wave penetration. Using the trend of the temperature elevation data in this region, the maximum SAR at the skin surface can be calculated with the following equation.

$$\mathrm{SAR} = \frac{\partial T(t)}{\partial t}\Big|_{t=0} \quad (2)$$

Then, the maximum transmitted power density can be derived as that of normal incidence of plane wave exposure using the following equation,

$$TPD_{est} = \frac{\rho \mathrm{SAR}}{\sigma} Re\left[\frac{1}{Z_p{}^*}\right] \quad (3)$$

where Z_p indicates the complex impedance of the phantom.

3. Results

Figure 2 shows the measured results of temperature elevation at phantom surface for cases of using standard horn, 2×2, 4×4, and 2×8 patch array antennas at 60 GHz, which have the maximum radiation gains of 21 dBi, 12 dBi, 17.4 dBi, and 17.0 dBi, respectively. The elevation trends of measured temperature data from 0 to $T(\tau)$ are fitted using the least squares method (LMS), where τ is determined by using (1). Since a long time of exposure will result in a variation of phantom state, such as the evaporation of moisture and shape change, the temperature at t = 360 s (6 min for averaging SAR [2], [3]) is considered as the T_{max}, i.e. steady-state of heat transfer.

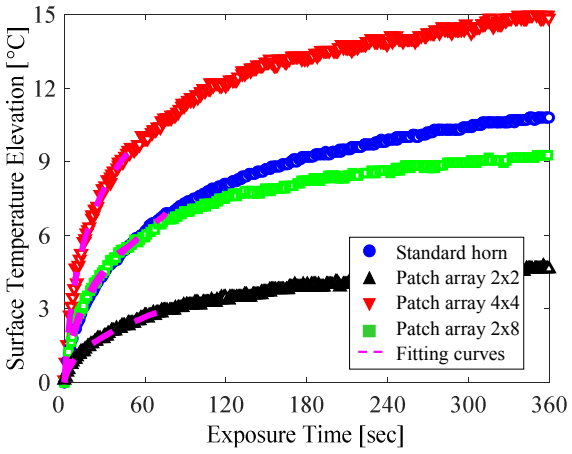

Figure 2. Surface temperature elevation of phantom by using different types of antennas at 60 GHz with antenna input power normalized to 1W.

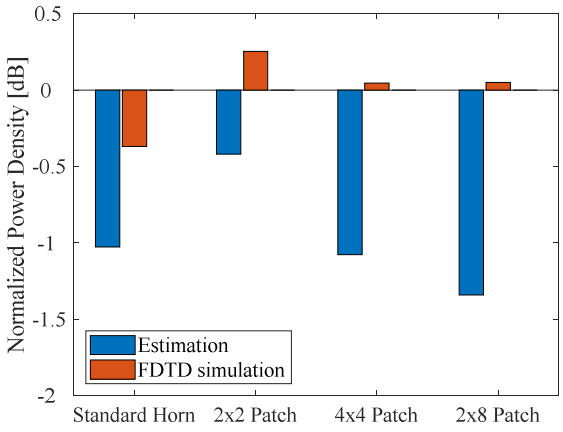

Figure 3. Maximum transmitted power density normalized to that of plane wave incidence for different types of antennas derived by the proposed estimation method and FDTD simulation.

Figure 3 shows the results of maximum transmitted power density at phantom surface for cases of four antennas in the experiment. For comparison, the results carried out by FDTD (Finite-difference time-domain) simulation are also included. In addition, the theoretical values of plane wave incidence situation are also calculated by the following equation,

$$TPD_{pw} = IPD \cdot \cos\theta_i \,(1 - |\Gamma|^2) \qquad (4)$$

where *IPD* denotes the peak value of incident power density in each case. The incident power density distribution is derived using the plane wave spectrum expansion method (PWS) based on the measurement data of electric field [6]. θ_i, which denotes the incident wave angle from air to phantom surface, is set to 0 in this study. Γ indicates the complex reflection coefficient from the phantom surface into the air.

As shown in figure 3, compared to the analytical results, the proposed method shows an underestimation of the transmitted power density in each case of antenna. The estimated results have the difference of 21.1%, 9.2%, 21.9%, and 26.6% for cases of standard horn, 2×2, 4×4, and 2×8 patch arrays, respectively, compared with the theoretical values of plane wave exposure scenarios. While the difference of estimated results and FDTD simulations are 14.1%, 14.3%, 22.8%, and 26.6% for cases of above-mentioned antennas, respectively.

In figure 3, the difference less than 10% between the proposed estimation method and the analytical approaches using 2×2 patch can be observed. For other antenna cases, the differences are increased up to 26%. Considering a large uncertainty of temperature experiment, the proposed method gives a reasonable and acceptable estimation results of the maximum transmitted power density. The main reason of large difference can be attributed to different antenna beams width, which eventually results in different radio wave penetration patterns inside the phantom. Thus, it is expected to clarify the correlation between the transmitted power density and temperature elevation by analyzing the impact caused by antenna beam width, i.e. exposed area.

4. Discussion

Figure 4 shows the heating potential of the incident and transmitted power density as a function of avereging area for different types of antennas using FDTD simulation. The heating potential is defined as the required power density to obtain 1◦C temperature elevation over the phantom surface [8], i.e., derived by the ratio of power density to the maximum temperature elevation T_{max} using the equipment in figure 1. The incident power density (*IPD*) is obtained by using PWS method, while the transmitted power density (*TPD*) is based on FDTD simulation.

As shown in figure 4, when the 2×2 patch array antenna is used, the ratios of *IPD* and *TPD* to T_{max} performs almost flat profiles regardless of averaging areas, and also agree well with the results of plane wave incidence. On the other hand, when the exposed area is averaged to 1 cm^2, the heating potential of power densities show the differences within 0.25 dB in both incidence and transmission cases. The fact indicates that the 1 cm^2 exposed area that should be averaged [4] is also appropriate for evaluating the transmitted power density.

Figure 5 shows the normalized incident and transmitted power density on *xy*-plane using the above-mentioned types of antennas. As can be seen in figure 5, the 2×2 patch array exhibits a near uniform distribution in both *TPD* and *IPD*. This fact explains the reason why the heating potential of *TPD* using 2x2 patch array agrees well with that of plane wave exposure, as shown in figure 4. On the other hand, owing to the narrow beam widths, the heating potential of horn, 2×8 and 4×4 patch arrays degrade when the averaging area is larger than 1 cm^2. Moreover, the relative distribution of *TPD* of these antennas does not change owing to a high radiation gain, i.e. shrill penetration pattern. On the other hand, the 3-dB beam width of the 2×2 patch array degrades obviously from *IPD* to *TPD*.

Table 2 shows the statistical distribution of the transmitted power density inside the phantom surface. It can be observed that 2×2 patch array performs a wide range of exposure intensity at the 3-dB and 5-dB regions than other antennas. This will result in a large lateral extent of *TPD* inside the phantom, leading to lower thermal gradients at the phantom surface, and thus the thermal response time of the surface temperature will be longer [9]. In order to improve the accuracy of our proposed method, it is necessary to clarify the relationship between transmitted power density and temperature elevation by determining the appropriate antenna beam width and penetration pattern. This will be addressed in future studies.

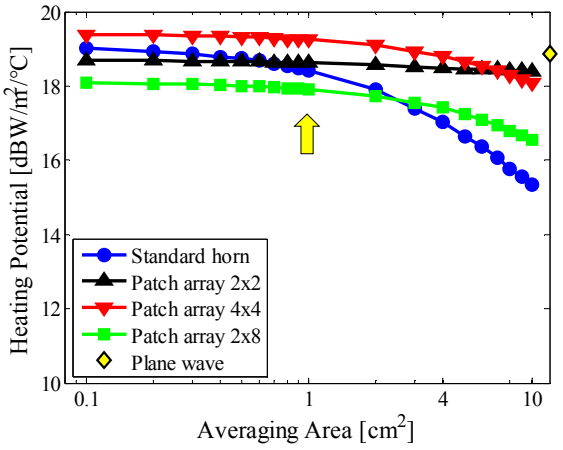

(a)

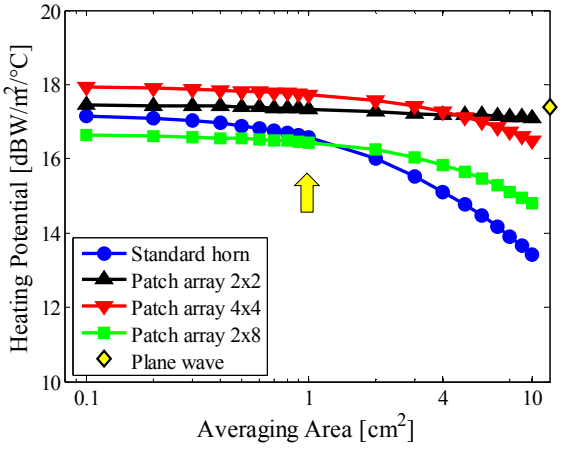

(b)

Figure 4. Ratio of incident and transmitted power density to maximum temperature elevation as a function of averaging area using different types of antennas, (a) *IPD* / T_{max}, (b) *TPD* / T_{max}.

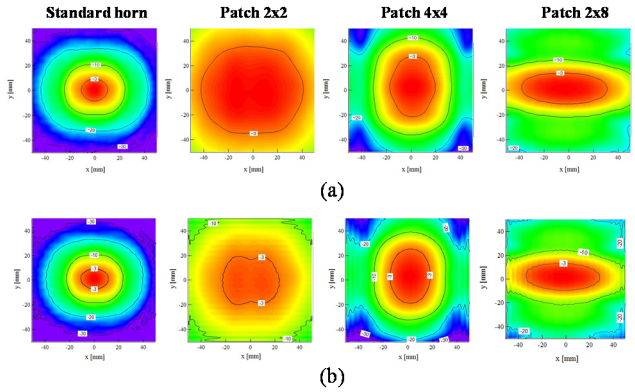

(a)

(b)

Figure 5. Normalized power density distrubtion in xy-plane using standard horn, patch 2x2, patch 4x4 and patch 2x8, (a) Incident power density, (b) Transmitted power density.

Table 2. Statistical distribution of the transmitted power density inside phantom surface at 60 GHz

	Max.-to-Min.	3-dB	5-dB
Horn	39.4 dB	9.6 %	17.4%
2×2 Patch	15.2 dB	56.8%	77.2%
4×4 Patch	38.6 dB	14.6%	23.0%
2×8 Patch	28.0 dB	18.9%	38.3%

6. Acknowledgements

This work was partly supported by the Ministry of Internal Affairs and Communications, Japan.

7. References

1. T. S. Rappaport, S. Sun, R. Mayzus, H. Zhao, Y. Azar, K. Wang, G. N. Wong, J. K. Schulz, M. Samimi, and F. Gutierrez, "Millimeter wave mobile communications for 5G cellular: It will work!" IEEE Access, vol. 1, no. 1, pp. 335-349, 2013.

2. IEEE Standard for Safety Levels with Respect to Human Exposure to the Radio Frequency Electromagnetic Fields, 3 kHz to 300 GHz, IEEE Std., C95.1, 2005.

3. ICNIRP Guidelines, "Guidelines for limiting exposure to time-varying electric, magnetic, and electromagnetic fields (up to 300 GHz)," Health Phys., vol. 74, pp. 494-522, 1998.

4. Y. Hashimoto, A. Hirata, R. Morimoto, S. Aonuma, I. Laakso, K. Jokela, and K. R. Foster, "On the averaging area for incident power density for human exposure limits at frequencies over 6 GHz," Phys. Med. Biol., vol. 62, no. 8, pp. 3124-3138, 2017.

5. ICNIRP Guidelines Draft Ed. 2018, "Draft guidelines for limiting exposure to time-varying electric, magnetic, and electromagnetic fields (up to 300 GHz)".

6. K. Kawabata, K. Li, K. Sasaki, R. Suga, S. Watanabe, and O. Hashimoto, "An Assessment of Surface Temperature Elevation of a Phantom for Exposure at 60 GHz", IEICE Technical Report, EMCJ2017-82, Dec. 2017.

7. R. Morimoto, A. Hirata, I. Laakso, M. C. Ziskin, and K. R. Foster, "Time constants for temperature elevation in human models exposed to dipole antennas and beams in the frequency range from 1 to 30 GHz," Phys. Med. Biol., vol. 62, no. 5, pp. 1676-1699, 2017.

8. K. Li, K. Sasaki, and S. Watanabe, "Heat Potential of Power Density for MMW Exposure Assessment from 6 GHz to 1 THz", PIERS2018, p. 222, Toyama, Aug. 2018.

9. K. R. Foster, A. Lozano-Nieto, P. J. Riu and T. S. Ely, "Heating of Tissues by Microwaves: A Model Analysis," Bioelectromagnetics, vol. 49, no. 7, pp. 420-428, 1998.